Electronic structure and crystal chemistry of niobium oxide phases

S. A. Turzhevsky
Institute of Solid State Chemistry, Ekaterinburg, Russia

D. L. Novikov, V. A. Gubanov, and A. J. Freeman
Materials Research Center and Department of Physics and Astronomy, Northwestern University, Evanston, Illinois 60208
(Received 14 January 1994)

Results of local-density linear muffin-tin orbital (LMTO) electronic-structure calculations for both known and recently obtained niobium oxide phases with different crystal lattices and different coordination of Nb atoms are presented. Perovskite-like compounds with one- or two-dimensional Nb-O condensed clusters, as well as hexagonal layered structures with trigonal-prismatic coordination of Nb atoms, are used. For $SrNbO_3$, $BaNb_5O_8$, $BaNb_4O_6$, and $Sr_2Nb_5O_9$, the Fermi level is located at the shoulder of the Nb d conduction band with a low density of oxygen states. For hexagonal M_xNbO_2 (M = Li, Na) compounds, oxygen contributions definitely appear at E_F, but remain small compared with those of the high-T_c superconducting cuprates. Pair-interaction energies and superexchange-interaction parameters were calculated using the LMTO Green-function method. Typical for high-T_c superconductors, antiferromagnetic coupling between metal atoms in the Nb-O planes is shown to exist, but not the ferromagnetic exchange between metal d and oxygen p states. The calculations show that perovskite niobium oxide systems are not good candidates in the search for new high-T_c superconducting materials, but that hexagonal layered niobium oxide phases of the type considered in this paper might be of interest in studies of low T_c superconducting oxides.

I. INTRODUCTION

The discovery of high-T_c superconductivity in copper oxides and their rapid elaboration by both solid-state synthesis techniques and experimental investigations of their various physical and chemical properties has served to greatly increase interest in the study of a wide variety of other transition metal-oxide systems. In particular, niobium oxide compounds are very interesting because they possess very rich crystal chemistry (e.g., they may contain Nb atoms in variable oxidation states), show distinct Jahn-Teller distortions, different Nb coordinations, form both high- and low-dimensional niobium oxygen networks, contain condensed clusters and permit the existence of different intergrowth phases.[1-3] All these properties are the basis for a belief that some superconducting phases may exist in niobium oxide systems, but that they are either highly unstable or are formed in very small quantities under typical experimental conditions.

Unusual temperature-dependent resistivity and magnetic susceptibility anomalies for some systems containing niobium have been observed[4,5] and interpreted as the possible appearance of high-T_c superconducting properties. Some poorly reproducible experimental indications on the possible presence of superconducting La-Sr-Nb-O phases in niobium oxide films have been reported.[4] The partial substitution of Cu for Nb in $YBa_2(Cu_{1-x}Nb_x)_3O_{7-\delta}$ and $Y_{0.6}Ba_{0.4}(Cu_{1-x}Nb_x)O_{2+y}$ does not destroy superconductivity over rather wide concentration limits, shows sufficient "compatability" of Nb with superconducting characteristics, and tends to decrease the width of the superconducting transition temperature with a simultaneous increase in the Meissner effect in the ceramics studied.[6]

Recently, low-temperature superconductivity was observed in Li_xNbO_2 compounds[7] which contain niobium in trigonal-prismatic coordination. The low-field magnetic susceptibility of this compound reaches diamagnetic values at $T=5.5$ K for $Li_{0.45}NbO_2$, and $T=5$ K for $Li_{0.5}NbO_2$. Although these values are much lower than the $T_c=13.7$ K obtained for the lithium-titanium spinel, $LiTiO_2$,[8] they do provide evidence that superconductivity is possible in niobium oxide phases.

In this paper, we present results of theoretical modeling of the electronic structure for a number of niobium oxide compounds with different crystal lattices and Nb oxidation states using the linear muffin-tin orbital (LMTO) method. The total and partial densities of states at the Fermi level, energies of covalent bonding and superexchange-interaction parameters are determined and compared with the relevant results for the high-T_c superconducting copper-oxide systems and the known low-temperature oxide superconductors.

II. CRYSTAL STRUCTURES

We have studied two groups of niobium oxide compounds:

(a) the recently discovered perovskite-like $BaNb_4O_6$, $BaNb_5O_8$, and $Sr_2Nb_5O_9$ phases as compared with the known $SrNbO_3$ compound; these are typical phases in the M-Nb-O system with M being divalent or trivalent metals with Nb oxidation numbers between 4+ and 2.5+;

(b) hexagonal layered $LiNbO_2$, $Li_{0.5}NbO_2$, and $NaNbO_2$ compounds with Nb oxidation between 3+ and 3.5+.

The crystal structure of $SrNbO_3$ is the simple perovskite lattice[9] with a lattice constant of 4.024 Å [Fig. 1(a)]. Other compounds from subgroup (a) are the intergrowth phases, typical ones being $Ba_2Nb_5O_9$ (Ref. 10) or $Ba_2Nb_5O_9$ (Ref. 11) [Fig. 1(b)]. For example, the latter can be described as an ordered intergrowth of alternating layers of $BaNbO_3$ (or $SrNbO_3$) perovskite and NbO (ordered deficient $B1$-type structure); its space group is $P4/mmm$, and the unit-cell parameters are $a=4.166$ Å and $c=12.215$ Å.[12] The atomic coordinates for the $Ba_2Nb_5O_9$ unit cell are given in Table I. Each Nb atom in the perovskite layer is coordinated by six oxygens as in $BaNbO_3$, four of which are shared with the neighboring NbO_6 octahedron of the perovskite layer. Two remaining oxygen atoms are also bonded with Nb atoms in the NbO layer, which can be described as condensed Nb_6O_{12} clusters, similar to that in NbO.[13] The Nb atoms in these clusters form regular Nb_6 octahedra, with a Nb-Nb distance of 2.94 Å, as compared with 2.97 Å in NbO. As a result, there are three nonequivalent types of metal atoms: four-coordinated Nb(1) (planar coordination by four oxygens, with Nb-O bond lengths=2.36 and 2.085 Å) a five-coordinated Nb(2) [square pyramid with r(Nb-O) =2.10 and 2.16 Å], and Nb(3) atoms coordinated by six oxygens of two nonequivalent groups (Nb-O bond lengths are 2.085 and 1.87 Å). It is worth noting that the crystal structure of this phase is rather similar to the tetragonal modification of $YBa_2Cu_3O_{7-y}$.

The crystal structure of $BaNb_4O_6$ is closely related to that of $Ba_2Nb_5O_9$, but differs by the thickness of the perovskite-like layer. If one writes the general formula as $n(BaNbO_3)\cdot 3(NbO)$, then $Ba_2Nb_5O_9$ is the intergrowth phase with doubled thickness of perovskite-like layer ($n=2$) and $BaNb_4O_6$ corresponds to the $n=1$ case (single perovskite-like layer). Both of these phases, $n=1$ and $n=2$, contain two-dimensional condensed niobium oxide clusters (see above). The space group of the $BaNb_4O_6$ crystal lattice is $P4/mmm$, with lattice parameters $a=4.169$ Å, $c=8.196$ Å.[11] In this lattice Nb(1) atoms are still four coordinated, and the Nb (2) atoms are coordinated by six oxygens; unlike $Ba_2Nb_5O_9$, five-coordinated Nb does not appear. The oxygen atoms are split into three nonequivalent types [Fig. 1(c)]; the coordinates of the atoms in the unit cell are given in Table I.

Unlike the phases considered above, $BaNb_5O_8$ contains only one-dimensional condensed niobium oxide clusters and has two nonequivalent types of Nb atoms: four-coordinated Nb(1) and five-coordinated Nb(2), with two nonequivalent types of oxygens: O(1) and O(2) [see Fig. 1(b)]. The typical Nb-Nb distance in this structure is 2.9 Å, the Nb-O distance is 2.1 Å.[10] The crystal has the space group $P4/m$, the unit cell contains one formula unit, and the lattice parameters are $a=6.608$ Å and $c=4.107$ Å; the atomic coordinates in the unit cell are given in Table I.[11]

According to the available experimental data, these compounds are similar to other related niobium oxide phases previously studied,[14,15] reveal metallic conductivity and a temperature-dependent resistivity typical for metals (Fig. 2). The resistivity essentially increases with

TABLE I. Atomic coordinates in the unit cells of niobium oxide phases.

$BaNb_5O_8$, $P4/m,z=1$				$BaNb_4O_6$, $P4/mmm,z=1$			
Atom	X	Y	Z	Atom	X	Y	Z
Ba	0.0	0.0	0.0	Ba	0.0	0.0	0.0
Nb(1)	0.5	0.5	0.0	Nb(1)	0.5	0.0	0.5
Nb(2)	0.4047	0.2094	0.5	Nb(2)	0.5	0.5	0.2467
O(1)	0.3929	0.3034	0.0	O(1)	0.5	0.5	0.0
O(2)	0.0986	0.3001	0.05	O(2)	0.5	0.0	0.2442
				O(3)	0.0	0.0	0.5
$Sr_2Nb_5O_9$, $P4/mmm,z=1$				$LiNbO_2$, $P6/3,z=2$			
Atom	X	Y	Z	Atom	X	Y	Z
Sr	0.0	0.0	0.1661	Li(1)	0.0	0.0	0.0
Nb(1)	0.0	0.5	0.5	Li(2)	0.0	0.0	0.5
Nb(2)	0.5	0.5	0.3351	Nb(1)	$\frac{1}{3}$	$\frac{2}{3}$	$\frac{3}{4}$
Nb(3)	0.5	0.5	0.0	Nb(2)	$\frac{2}{3}$	$\frac{1}{3}$	$\frac{1}{4}$
O(1)	0.5	0.0	0.0	O(1)	$\frac{1}{3}$	$\frac{2}{3}$	0.1263
O(2)	0.5	0.5	0.1598	O(2)	$\frac{2}{3}$	$\frac{1}{3}$	0.8737
O(3)	0.5	0.0	0.3272	O(3)	$\frac{2}{3}$	$\frac{1}{3}$	0.6263
O(4)	0.0	0.0	0.5	O(4)	$\frac{1}{3}$	$\frac{2}{3}$	0.3737

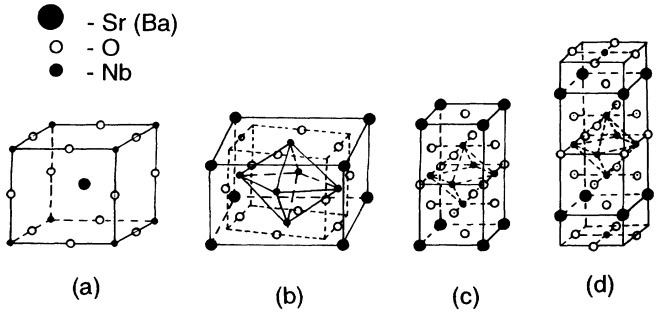

FIG. 1. Crystal structure of niobium oxide compounds: (a) $SrNbO_3$; (b) $BaNb_5O_8$; (c) $BaNb_4O_6$; (d) $Ba_2Nb_5O_9$.

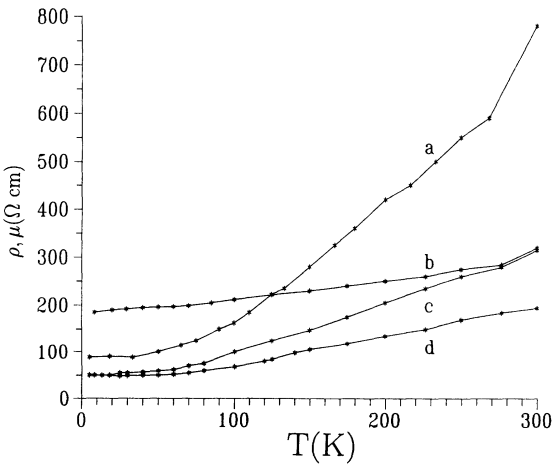

FIG. 2. Temperature dependences of the electrical resistivity for (a) $BaNb_5O_8$, (b) $Ba_2Nb_5O_9$, (c) $BaNb_6O_{9.4}$, (d) $BaNb_4O_6$, (e) $BaNb_8O_{14}$.

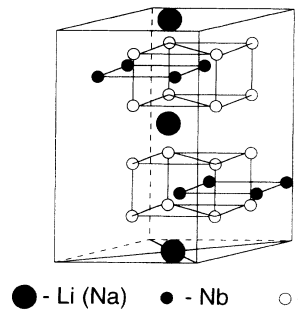

FIG. 3. Crystal structure of hexagonal $LiNbO_2$.

the lowering of dimensionality of niobium oxide cluster networks: from deficient niobium monoxide (containing 25% of oxygen vacancies) with three-dimensional Nb-O clusters, to $BaNb_4O_6$ or $Ba_2Nb_5O_9$ with two-dimensional Nb-O clusters, and further to $BaNb_5O_8$ with a one-dimensional condensation of niobium oxide clusters.

The layered intercalated Li_xNbO_2 and Na_xNbO_2 phases obtained recently are of a completely different crystal structure type. The layered $LiNbO_2$ (Ref. 16) crystal lattice contains hexagonal planes of Nb atoms, separated by hexagonal oxygen layers (Fig. 3). The unit cell contains two types of nonequivalent Nb atoms; both are in trigonal-prismatic coordination. Lithium occupies octahedral sites between oxygen-niobium-oxygen layers. The space group of the lattice is $P6\{3\}$ and its lattice parameters are $a=2.905$ Å, $c=10.46$ Å.[16] Atomic coordinates for a doubled unit cell are given in Table I. A similar crystal lattice was observed for $NaNbO_2$[17] with lattice parameters: $a=2.958$ Å; $c=11.58$ Å; $z_0=0.135$. When calculating the nonstoichiometric phases, we kept the lattice parameters unchanged; thus, the relaxation of the lattice was not taken into account when alkali-metal vacancies are present.

III. COMPUTATIONAL METHODS

The electronic structure of $SrNbO_3$, $BaNb_4O_6$, $BaNb_5O_8$, $Sr_2Nb_5O_9$, Li_xNbO_2, and $NaNbO_2$ was calculated using the linear muffin-tin orbital–atomic sphere-approximation (LMTO-ASA) method[18] with the Hedin-Lundqvist form[19] for the exchange-correlation potential. Atomic-sphere radii were varied through the self-consistency procedure in accordance with the electroneutrality condition.

In order to study chemical bonding and magnetic interactions in some of these compounds in more detail, we have used the tight-binding approximation,[20] which allows an analysis of these parameters for different orbitals and different atoms in real space. As shown in Ref. 21, the most important contribution to the cohesive energy of the crystal is the covalent interaction energy, which describes the lowering of the total energy due to the interactions between atoms and is the nondiagonal part of the total band energy

$$E_{(\mathrm{cov})}=\sum_{i\neq j}\sum_{LL'}N^{ij}_{LL'}H^{ij}_{LL'} \ . \tag{1}$$

Here $H^{ij}_{LL'}$ is the real space two-center tight-binding Hamiltonian[20] and $N^{ij}_{LL'}$ is the occupation of the bond formed by the orbital $L(l,m)$ of the ith atom and the orbital $L'(l'm')$ of the jth atom. The $N^{ij}_{LL'}$ matrix can be easily determined through the Green function $G^{ij}_{LL'}(E)$:

$$N^{ij}_{LL'}=\frac{1}{\pi}\mathrm{Im}\int_{-\infty}^{E_F}G^{ij}_{LL'}(E)dE \ . \tag{2}$$

The nondiagonal Green function $G^{ij}_{LL'}(E)$ is readily calculated from the LMTO band-structure results, i.e., the one-electron energy spectrum $E_n(k)$ and the wave functions $\psi_{nL}(\mathbf{k})$ of the LMTO Hamiltonian

$$G^{ij}_{LL'}=\frac{1}{\Omega_{\mathrm{BZ}}}\int d\mathbf{k}\sum_n\frac{\psi_{nL}(\mathbf{k})\psi^*_{nL'}(\mathbf{k})}{E-E_n(\mathbf{k})}e^{i\mathbf{k}\mathbf{R}_{ij}} \ . \tag{3}$$

Thus, the energy of a separate chemical bond, $E^{ij}_{LL'}$, is just the product of the occupancy of the band $N^{ij}_{LL'}$ (which can vary between 0 and 1) and the maximum energy of the bond $H^{ij}_{LL'}$. If $H^{ij}_{LL'}$ is negative, then $N^{ij}_{LL'}>0$ corresponds to the bonding interaction of the orbital L of the ith atom with orbital L' of the jth atom, and $N^{ij}_{LL'}<0$ describes the antibonding interaction when H is positive. The diagonal part N^{ij}_{LL} is always positive and gives the number of electrons in the state iL.

The character of the bonding between the orbitals iL and jL' at the Fermi level can be described by the following part of the nondiagonal density of states:

$$n^{ij}_{LL'}=\frac{1}{\pi}\mathrm{Im}G^{ij}_{LL'}E_f \ . \tag{4}$$

The square of the $n^{ij}_{LL'}=\langle\psi^i_L I\psi^j_{L'}\rangle$ value gives the probability of electron transfer between these orbitals.

In the scope of these approximations, one can also define a simple way to estimate the exchange-interaction parameters of the effective Heisenberg Hamiltonian

$$H_{\mathrm{ex}}=-\frac{1}{2}\sum_{ij}J_{ij}\mathbf{S}_i\mathbf{S}_j \ . \tag{5}$$

As found in Ref. 22, in the case of small magnetic moments using perturbation theory and the local force theorem, one can determine the energy changes connected with small deviations in the direction of the magnetic moment. These changes are given by the relation

$$\Delta E=-\frac{1}{4}\sum_{ij}\sum_{LL'}I_iI_jX^{ij}_{LL'}\mathbf{m}_i\mathbf{m}_j \ , \tag{6}$$

where $X^{ij}_{LL'}$ is the nonlocal magnetic susceptibility

$$X^{ij}_{LL'}=\frac{1}{\pi}\mathrm{Im}\int_{-\infty}^{E_F}dE\ G^{ij}_{LL'}(E)G^{ji}_{LL'}(E) \tag{7}$$

and the effective exchange integrals values in Eq. (5) can be easily found as[22]

$$J_{ij}=\frac{1}{2}\frac{I_i\cdot I_j}{S_i\cdot S_j}\sum_{LL'}x^{ij}_{LL'} \tag{8}$$

Here I_j is the intra-atomic exchange parameter for the

ith atom. It is worth noting that due to the sharp dependence of $G^{ij}_{LL'}$ on the energy, the integral (7) has to be calculated as a contour integral over the complex plane. As seen from Eqs. (7) and (8), in such a definition the exchange integral does not contain any adjustable parameters and can be calculated directly from the LMTO band-structure results, which take into account all chemical bonding effects.

Unlike the perovskite-like compounds, hexagonal phases with trigonal-prismatic coordination of Nb atoms are less closely packed and, as our preliminary calculations showed, the errors encountered by the use of the LMTO-ASA method could be rather substantial and so distort the shape of the conduction bands. In order to overcome this difficulty for Li_xNbO_2 and Na_xNbO_2, we have used the full-potential LMTO (FLMTO) method,[23] which does not invoke any shape approximation on either the potential or the charge density for the valence states and so is well suited to treat low-symmetry structures. We used the triple-κ basis set for each type of atom and each angular momentum l channel (l up to 3) with kinetic energies -0.7, -1.0, and -2.3 Ry. The muffin-tin (MT) sphere radii were chosen to be $R(\mathrm{Nb})=1.79$, $R(\mathrm{O})=2.20$, $R(\mathrm{Li})=1.80$ for Li_xNbO_2, and $R(\mathrm{Nb})=1.88$, $R(\mathrm{O})=2.20$, $R(\mathrm{Na})=2.16$. The Brillouin-zone integrations were carried out using a 170 k-point mesh by the tetrahedron method for stoichiometric compounds and 260 k points for the crystals with vacancies.

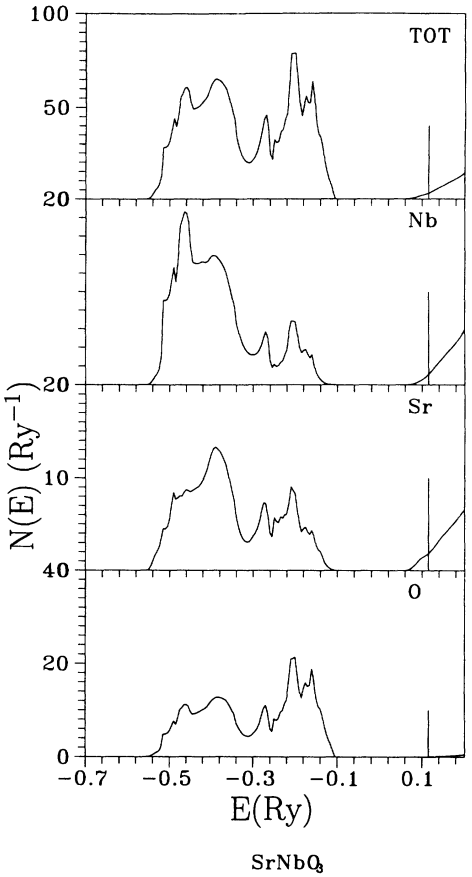

FIG. 4. Total and partial densities of states for $SrNbO_3$.

IV. RESULTS AND DISCUSSION

A. $SrNbO_3$

The total and partial densities of states for the simple perovskite $SrNbO_3$ are shown in Fig. 3. As seen, they present ideal stoichiometric $SrNbO_3$ as a poor metal: the Fermi level falls on the shoulder of the conduction band composed mainly of Nb d states. The gap between the valence and conduction bands is about 0.17 Ry and the occupied conduction bandwidth is 0.087 Ry. There is significant hybridization of Nb d and oxygen $2p$ states in the valence band (its width is 0.45 Ry); the main contribution to the lower part of the valence band comes from Nb, and the upper part is formed predominantly from the oxygen $2p$ states. As is known from the experiments, $SrNbO_3$ crystals may show metallic, semiconducting, or insulating behavior depending on Sr and O stoichiometry as well as synthesis conditions.[24,25] This can be understood from the calculated results (Fig. 3) if, as a first approximation, one uses the rigid-band model and follows the shifts of E_F with valence-electron concentration.

B. $BaNb_4O_6$, $Sr_2Nb_5O_9$, and $BaNb_5O_8$

The electronic structure of the intergrowth phases $BaNb_4O_6$ and $Sr_2Nb_5O_9$ with two-dimensional niobium oxygen clusters is more complicated (cf. Figs. 4 and 5). The crystal structures of these two compounds are rather similar, but the latter contains two Nb-O clusters instead of the single one in $BaNb_4O_6$ (see Sec. II). The calculated density of states (DOS) are similar for both: the Fermi level falls on the slope of the conduction band formed predominantly by contributions from Nb $4d$ states. The oxygen state contributions at E_F are very small (see Table II), and these compounds are poor metals, in agreement with the data in Fig. 2. Niobium atoms, especially in $Sr_2Nb_5O_9$, are highly nonequivalent, with Nb(3) atoms almost not participating in the conductivity; their d states

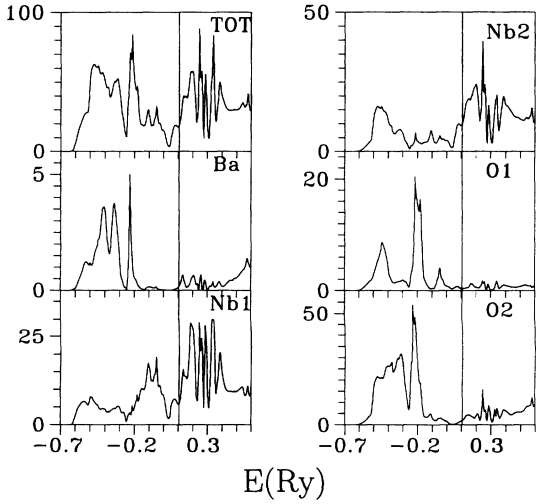

FIG. 5. Total and partial densities of states for $BaNb_4O_6$.

are located above E_F. The data in Table II show that the increase of the number of Nb-O clusters results in the sharp increase of the $N(E_F)$ value. A significant oxygen [O(4)] contribution to $N(E_F)$ appears for $Sr_2Nb_5O_9$, which is missing in $BaNb_4O_6$. Fivefold coordinated Nb(2) atoms are much more involved in conductivity than Nb(1), and especially Nb(3), which should make the electrical characteristics of this compound strongly anisotropic. In this sense, the composition of metal states at E_F for $BaNb_4O_6$ is much more uniform: the contributions of both Nb(1) and Nb(2) atoms are close, though two times less than in $Sr_2Nb_5O_9$; the small oxygen contributions are very small and comparable in value; the Ba contributions are negligible.

The structure of the DOS below E_F for these intergrowth phases is typical of d-metal oxides: there is essential mixing of Nb $4d$ and O $2p$ states, and the valence bands of both oxides are heavily hybridized. But, in the upper part of the valence-band hybridization is almost entirely missing, and the electronic states are almost purely O $2p$ states, in sharp contrast with the copper-oxide superconductors. The upper edge of the O $2p$ band is located 0.3 Ry below E_F in $BaNb_4O_6$. For $Sr_2Nb_5O_9$, the states of different nonequivalent oxygens are located at different energies below E_F, from 0.27 Ry for O(4) down to 0.47 Ry for O(1).

Thus, there are hardly any similarities between the peculiarities of electronic state distributions in the intergrowth $BaNb_4O_6$ and $Sr_2Nb_5O_9$ phases and the Cu-O high-T_c, which could give an indication of similar superconductivity mechanisms existing in these Nb-O compounds. This is also true for $BaNb_5O_8$ with its one dimensional niobium oxide clusters whose DOS are shown in Figs. 6 and 7 and whose $N(E_F)$ values are listed in Table II. The Fermi level is situated in the region with a very low DOS. The d-state contribution of five-coordinated Nb atoms is largest; the one from four coordinated Nb(1) is more than two times lower. The main hybridization between Nb d and O $2p$ states takes place well below E_F, with O(1) p states located in the upper

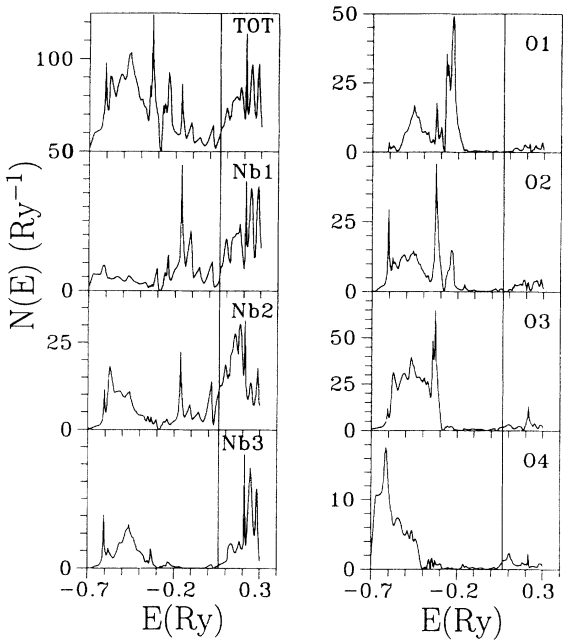

FIG. 6. Total and partial densities of states for $Sr_2Nb_5O_9$.

part of the valence band and O(2) p states mainly at the bottom. Ba atoms again do not give practically any contributions to the states close to E_F. The results obtained are in line with the experimental tendency discussed above (cf. Fig. 2) that the lowering of the niobium-monoxide cluster network dimensionality leads to the tendency of the resistivity to increase.

Table III presents the energies of covalent bonding calculated for $BaNb_4O_6$ and $BaNb_5O_8$. In the first, the bonding of six-coordinated Nb(2) with O(1) atoms is the strongest and results in the shortest Nb-O distance. The predominant contribution is the energy of the O(1)$2p$-Nb(2)p interaction; the energy of the Nb(2)d-O(1)$2p$ interaction is an order of magnitude less. Nb(2) atoms are

TABLE II. Total and partial densities of states at the Fermi level for $BaNb_5O_8$, $BaNb_4O_6$, $Sr_2Nb_5O_8$.

DOS (1/Ry)	$BaNb_5O_8$	$BaNb_4O_6$	$Sr_2Nb_5O_9$
Partial DOS:			
Ba or Sr	0.080	0.074	0.393
Nb(1)[a]	1.621	5.282	9.010
	(1.556)	(4.982)	(8.823)
Nb(2)[a]	4.229	4.848	12.632
	(4.191)	(4.712)	(12.246)
O(1)	0.423	0.282	
O(2)	0.495	0.384	0.282
O(3)		0.347	0.832
O(4)			1.592
Total DOS[b]	22.50	22.50	52.25

[a]d-state contributions are given in parentheses.
[b]The value per unit cell.

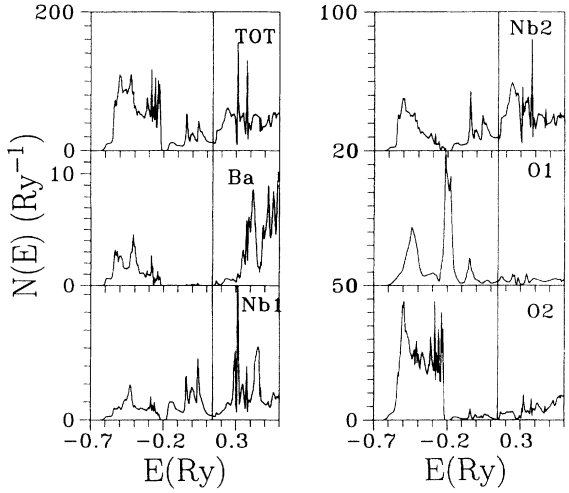

FIG. 7. Total and partial densities of states for $BaNb_5O_8$.

TABLE III. Energies of covalent bonding (E^{ij}) for $BaNb_5O_8$, $BaNb_4O_6$ (in mRy).

		$BaNb_4O_6$					
		Nb(1)			Nb(2)		
		s	*p*	*d*	*s*	*p*	*d*
O(1)	*s*				−31.1	−84.4	−36.9
	p				−78.9	−190	−17.4
O(2)	*s*	−0.7	−2.4	−1.3	−21.2	−1.24	−24.6
	p	−4.9	−13.2	−11.6	−1.77	−170	−14.1
O(3)	*s*	−4.6	0.0	−6.3			
	p	0.0	−47.2	−0.01			
		$BaNb_5O_8$					
O(1)	*s*	−1.2	−2.9	−1.1	−28.2	−0.5	−32.2
	p	−3.2	−8.1	−6.9	−0.4	−236	−0.4
O(2)	*s*				−13.4	−8.2	−3.5
	p				−7.3	−46.8	−14.3

less heavily bonded to the O(2) atoms, and, in contrast to that from O(1), the contribution of O(2)*p*-Nb(2)*s* interactions to the bonding energy is much less than for O(1) atoms. Four-coordinated Nb(1) is not so strongly bonded to the surrounding oxygens: the energies of O(2)*p*-Nb(1)*p* and O(2)*p*-Nb(1)*d* bonding are small and close, but for the O(3)-Nb(1) interactions, O(3)*p*-Nb(1)*p* is again the strongest.

In $BaNb_5O_8$ the strongest bonding is between five-coordinated Nb(2) and O(1) atoms [the shortest distance is Nb(2)-O(1)], and the energy of Nb(2) bonding with O(2) is much smaller (see Table III). Again the largest bonding energy arises from the *p* states of niobium and *p* states of oxygen. Nb(1) atoms are very weakly bonded in this crystal, and the distances between them and the oxygens are the largest in the lattice. Ba atoms are weakly bonded and equal to all the oxygens. A comparison of the covalent bonding energies in $BaNb_5O_8$ with the ones calculated for $YBa_2Cu_3O_7$ (Ref. 24) shows that the interactions of *d*-metal states with *p* orbitals of oxygen in $BaNb_5O_8$ is much weaker than in $YBa_2Cu_3O_7$ (see the electron transfer energies in Table IV); as a result, any strong hydridization of these states at E_F is absent in the niobium oxide compounds.

The analysis of superexchange interactions carried out for $BaNb_4O_6$ (see Table V) reveals the antiferromagnetic exchange interaction[22] between the niobium atoms in the Nb-O planes [large and negative values of nonlocal susceptibilities, similar to Cu(2)-O-Cu(2) in $YBa_2Cu_3O_7$] characteristic for superconducting copper oxides. But there is no considerable ferromagnetic exchange between the *d*-metal and oxygen *p* states, the presence of which is often considered to be one of specific features of high-T_c superconductors.[26,27]

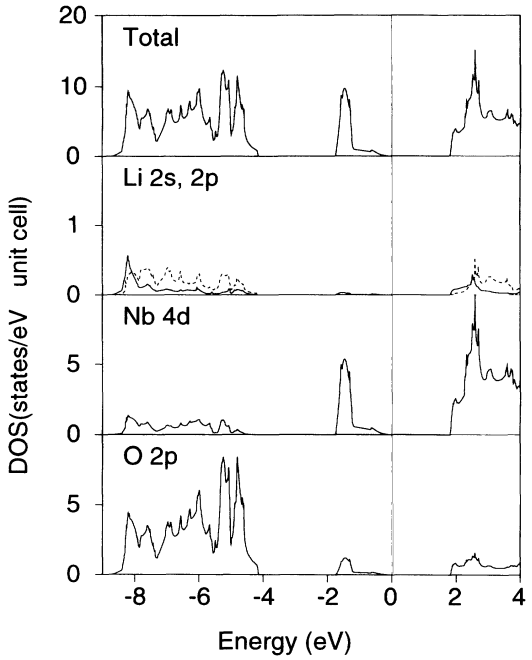

FIG. 8. Total and partial densities of states for hexagonal stoichiometric $LiNbO_2$.

Thus, we see that the distribution of electronic states, as well as the type of state hybridization, nature of states near E_F, chemical bonding parameters, and superexchange interactions in the simple $SrNbO_3$ perovskite and in the intergrowth phases with four-, five, or six-coordinated Nb considered above, are very different from the typical patterns of the known copper-oxide superconductors. Hence, these niobium oxide phases appear to be poor candidates for similar superconducting properties

C. Li_xNbO_2 and Na_xNbO_2

The situation appears to be different in the intercalated Li_xNbO_2 and Na_xNbO_2 phases (Fig. 3, Table I). Figure 8 gives the DOS in $LiNbO_2$ as calculated by the FLMTO method. In contrast to the perovskite-like phases considered above, a distinct gap of about 2 eV is seen between the valence and conduction bands, formed by the Nb 4*d* states with significant oxygen 2*p* contributions. Lithium appears to be completely ionized, neither 2*s* nor 2*p* states are mixed significantly with the valence or conduction bands, and the additional Li electron fills the conduction band, which appears to be completely oc-

TABLE IV. The probability of electron transfer between atoms in niobium oxide phases as compared with copper oxide superconductor.

$YBa_2Cu_3O_7$		$BaNb_5O_8$		$BaNb_4O_6$	
Cu(2)-O(2)	82.6	Nb(2)-O(2)	0.2	Nb(2)-O(1)	5.3
Cu(1)-O(4)	4.0	Nb(1)-O(1)	0.01	Nb(1)-O(2)	2.9
Cu(1)-O(1)	42.6	Nb(2)-O(1)	0.1	Nb(1)-O(1)	0.2

TABLE V. Nonlocal susceptibilities for $BaNb_4O_6$ as compared with the 123 copper oxide superconductor.

$YBa_2Cu_3O_7$	$\chi^{ij}_{dd(p)}$ (mRy^{-1})	$BaNb_4O_6$	$\chi^{ij}_{dd(p)}$ (mRy^{-1})
Cu(2)-O(2)-Cu(2)	−50.8	Nb(2)-O(3)-Nb(2)	−106.9
Cu(2)-O(3)-Cu(2)	−42.8	Nb(1)-O(3)-Nb(1)	−145.0
Cu(1)-O(4)-Cu(2)	−9.9	Nb(1)-Nb(2)	−5.4
Cu(1)-O(1)-Cu(1)	72.5	Nb(2)-Nb(2)	9.4
Cu(2)-O(2)	112.3	Nb(2)-O(1)	−3.1
O(2)-O(2)	35.5	Nb(2)-O(2)	−36.9

cupied for $LiNbO_2$. The vacant unoccupied part of the conduction band is well separated from the lower one by 1.5 eV. This energy diagram is surprisingly close to the early qualitative model suggested[28] from semiempirical extended Hückel calculations of an isolated NbO_2 layer, according to which the trigonal-prismatic coordinated Nb-O should be a nonmagnetic semiconductor with a gap of 1.4 eV. The experimentally observed antiferromagnetism was attributed there to impurity or nonstoichiometry effects.

As suggested in Ref. 7, the partial removal of Li should result in the gradual oxidation of the Nb atoms and the increase $N(E_F)$ due to the loss of electrons from the conduction band. Such a procedure was realized by the authors of Ref. 7: a hexagonal layered Li_xNbO_2 phase with $0.45 < x < 1.0$ was obtained which revealed the onset of superconductivity below 5.5 K. Later on, these results were also obtained in Ref. 29, where the synthesis procedure was changed and the detection of superconducting phases with T_c up to 12 K was claimed.

Using the FLMTO method, we also carried out the electronic-structure calculations for $Li_{0.5}NbO_2$ with 50% of Li vacancies. The computational parameters were kept the same as for the ideal crystal. The total and partial DOS are given in Fig. 9. As seen, E_F is located at the high-energy shoulder of the hybridized Nb $4d$–O $2p$ band, and $N(E_F)$ is rather high (Table VI). It is comparable with that found in the full linear-augmented plane-wave calculations for Li_2TiO_4 (Ref. 30) with $T_c = 13.7$ K, which definitely corresponds to the conventional electron-phonon type of superconductivity.[27] Definite similarities in the distribution of states and their nature near E_F are evident for both $Li_{0.5}NbO_2$ and $Li_{0.5}TiO_2$,[30] and lead to the expectation of a similar type of superconductivity in both crystals. The difference is in the location of the Fermi level; in $Li_{0.5}TiO_2$, E_F coincides with the maximum of a well-defined peak in the DOS curve.

TABLE VI. Total and partial densities of states in the MT spheres at the Fermi level for $Li_{0.5}NbO_2$, $Na_{0.5}NbO_2$, and the full potential augment plane wave results for $Li_{0.5}TiO_2$ (Ref. 30) (1/Ry, unit cell).

DOS	$Li_{0.5}TiO_2$	$Li_{0.5}NbO_2$	$Na_{0.5}NbO_2$
Li/Na		0.06	0.08
Nb		30.71	29.82
O		19.38	16.5
Total	43.0	81.9	73.6

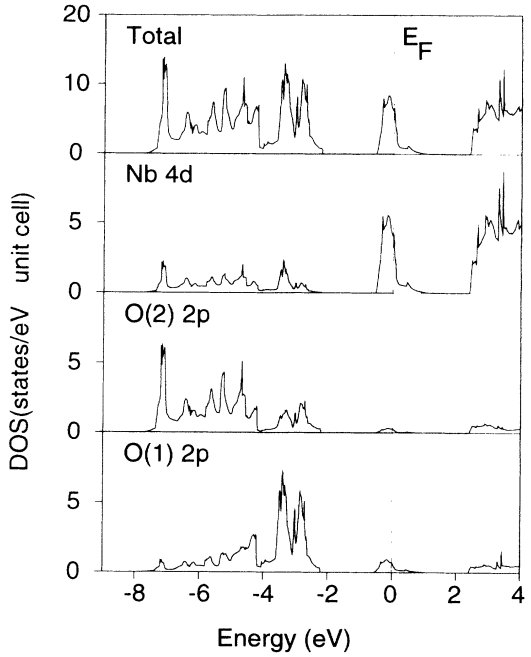

FIG. 9. Total and partial densities of states for hexagonal $Li_{0.5}NbO_2$.

As in electron-phonon superconductors, since the higher $N(E_F)$ corresponds to the higher T_c, one should not expect any increase of the T_c value with change of lithium content. In $Li_{0.5}NbO_2$, a further shift of E_F to the lower energy region, which can be reached by a decrease of Li in this hexagonal phase, might result in a substantial increase in $N(E_F)$, and consequently of T_c. Using the rigid-band model it is easy to show that the Fermi level will be located at the peak in the conduction band when

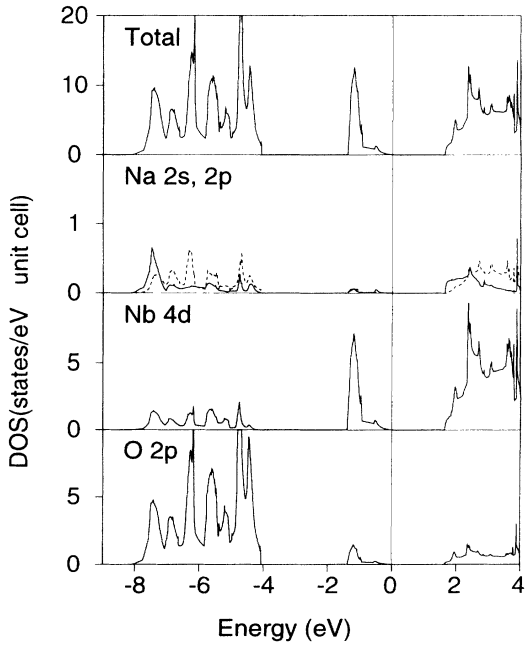

FIG. 10. Total and partial densities of states for stoichiometric $NaNbO_2$.

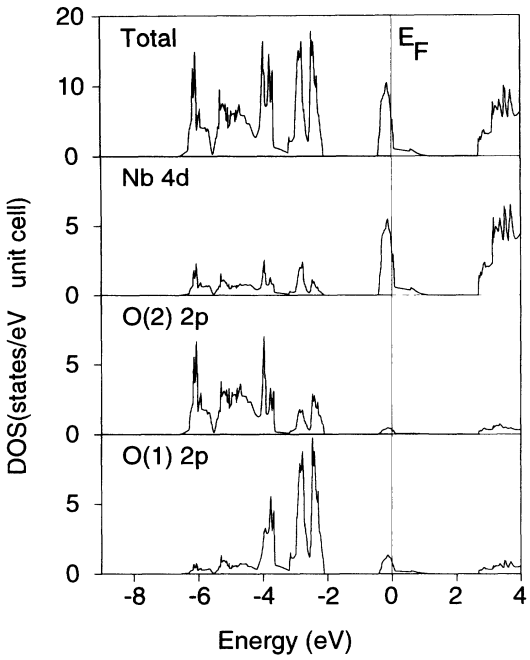

FIG. 11. Total and partial densities of states for $Na_{0.5}NbO_2$.

one more lithium atom is removed from the crystal lattice, i.e., for the hexagonal layered NbO_2 crystal with trigonal-prismatic coordination of Nb atoms. Indeed, such a phase, if it exists, has to be very unstable and is not known at the moment.

Similar results were obtained for ideal and nonstoichiometric Na_xNbO_2 crystals (cf. Figs. 10 and 11). The larger lattice parameters lead to a noticeable narrowing of both valence and conduction bands. The energy gap between them increases (up to 2.3 eV), the conduction bandwidth drops down to 1.35 eV in $NaNbO_2$ as compared with 1.8 eV in the $LiNbO_2$ case. When half of the Na atoms are removed from the crystal lattice, the Fermi energy is again located on the high-energy shoulder of the conduction band. Thus, $N(E_F)$ is rather high (Table VI) and this phase should become superconducting like $Li_{0.5}NbO_2$ with a comparable value of T_c. The relative contribution of O $2p$ states at E_F is about the same as in $Li_{0.5}NbO_2$, and the states which form the Cooper pairs are of predominantly d-metal type. From the absolute value of $N(E_F)$ one may expect that its T_c for $Na_{0.5}NbO_2$ will be of the same order of magnitude as for $Li_{0.5}NbO_2$ phase. But as the DOS peak near E_F is stronger and steeper, one may expect that the lowering of sodium content could result in more rapid changes in the T_c values in comparison with the Li_xNbO_2 system.

Thus, the calculated structure of the electronic states at E_F and other peculiarities of the calculated electronic distributions in Li_xNbO_2 and Na_xNbO_2 crystals, do not leave much doubt that the superconductivity of these compounds is of the usual electron-phonon origin, and completely different from that, if really observed, for some unknown niobium oxide phases in thin films.[4]

V. CONCLUSIONS

Results of the electronic-structure calculations for several known and possible phases in the M-Nb-O system (M is alkaline earth or alkaline metal) possessing different types of crystal structure, Nb coordination, and formal valencies, as well as different spatial dimensionalities of Nb-O networks, were carried out. The results obtained show that one can hardly expect the appearance of electronic-structure peculiarities specific for the known high-T_c copper-oxide materials, and hence, that the chances of finding any real high-T_c superconductors in the niobium oxide phases are low. At the same time, some specific types of Nb-O crystal lattices, such as the layered ones containing trigonal-prismatic coordinated Nb, may reveal conventional electron-phonon mediated low-temperature superconductivity with T_c of the order of 10 K when properly doped by alkali metals. The rich crystal chemistry of complex niobium oxide phases results in a wide variety of materials with different, and sharply changeable with composition, peculiarities of electronic structure, state distributions, chemical bonding, and magnetic and electric characteristics, which may be of great interest for application purposes.

ACKNOWLEDGMENTS

This work was supported by the MRL Program of the National Science Foundation at the Materials Research Center of Northwestern University, under Grant No. DMR-9120521, and a grant of computer time at Pittsburgh Supercomputing Center.

[1]C. N. R. Rao, *New Directions in Solid State Chemistry* (Cambridge University Press, Cambridge, England, 1986), p. 310.
[2]J. Kohler, A. Simon, S. J. Hibble, and A. K. Cheetham, J. Less-Comm. Metals **142**, 123 (1988).
[3]G. Swensson, Mater. Res. Bull. **23**, 437 (1988).
[4]T. Ogushi, S. Higo, N. G. Surecka *et al.*, J. Low Temp. Phys. **73**, 305 (1988).
[5]T. Ogushi, Y. Hakuraki, and T. Otawa, Jpn. J. Appl. Phys. **26**, 1141 (1987).
[6]N. G. Sureska, S. Higo, Y. Hakuraku *et al.*, Int. J. Mod. Phys. B **2**, 435 (1988).
[7]M. J. Geselbracht, T. J. Richardson, and A. M. Stacy, Nature (London) **345**, 324 (1990).
[8]D. C. Johnston *et al.*, Mater. Res. Bull. **8**, 777 (1973).
[9]D. Ridgley and R. Ward, J. Am. Chem. Soc. **77**, 6132 (1985).
[10]G. Swensson, Solid State Ionics **32/33**, 126 (1989).
[11]V. Zubkov, V. A. Perelyaev, I. F. Berger, and I. A. Kontsevaya (unpublished).
[12]V. G. Zubkov, V. A. Perelyaev, I. F. Berger, V. I. Voronin, I. A. Kontsevaya, and G. P. Shveikin, Dokl. Akad. Nauk SSSR **312**, 615 (1990) [Sov. Phys. Dokl. **35**, 399 (1990)].
[13]B.-O. Marinder, Chem. Scr. **18**, 169 (1981).

[14]V. G. Zubkov, V. A. Perelyaev, I. F. Berger, I. A. Kontsevaya, O. V. Makarova, S. A. Turzhevsky, V. A. Gubanov, V. I. Voronin, A. V. Mirmelstein, and A. E. Karkin, Superconductivity (Russia) **3**, 1969 (1990).

[15]V. Zubkov, V. A. Perelyaev, D. G. Kellerman, V. E. Startsev, V. P. Dyakina, I. A. Kontsevaya, O. V. Makarova, and G. P. Shveikin, Dokl. Akad. Nauk SSSR **313**, 367 (1990) [Sov. Phys. Dokl. **35**, 473 (1990)].

[16]G. Meyer and R. Hoppe, Angew. Chem. **86**, 819 (1974).

[17]G. Meyer and R. Hoppe, Z. Anorg. Chem. **424**, 128 (1976).

[18]O. K. Andersen, Phys. Rev. B **12**, 864 (1975).

[19]O. Gunnarsson and B. I. Lundquist, Phys. Rev. B **13**, 4274 (1976).

[20]O. K. Anderson and O. Jepsen, Phys. Rev. Lett. **53**, 2571 (1984).

[21]A. P. Sutton, M. W. Finnis, P. G. Pettifor, and Y. Ohta, J. Phys. C **21**, 35 (1988).

[22]V. A. Gubanov, S. A. Turzhevsky *et al.*, Physica C **153-155**, 123 (1988).

[23]M. Methfessel, Phys. Rev. B **38**, 1537 (1988).

[24]R. Kreiser and R. Ward, J. Solid State Chem. **1**, 368 (1970).

[25]D. Ridgley and R. Ward, J. Am. Chem. Soc. **77**, 6132 (1955).

[26]S. A. Turzhevsky, A. I. Lichtenstein, and V. A. Gubanov, *Electronic Structure and Chemical Bonding of High-T_c Superconductors* (Russia) (Ural Branch of USSR Academy of Science, Sverdlovsk, 1990), p. 45.

[27]V. V. Moschalkov and B. A. Popovkin, Zh. Vses. Khim. Ova. **34**, 19 (1989).

[28]J. K. Burdett and T. Hughbanks, Inorg. Chem. **24**, 1741 (1985).

[29]V. G. Zubkov, D. G. Kellerman, and G. P. Shveikin (unpublished).

[30]S. Massida, J. J. Yu, and A. J. Freeman, Phys. Rev. B **38**, 11 352 (1988).